

Accessing nanomechanical resonators via a fast microwave circuit

Mika A. Sillanpää,* Jayanta Sarkar, Jaakko Sulko, Juha Muhonen, and Pertti J. Hakonen
Helsinki University of Technology Low Temperature Laboratory Puumiehenkuja 2B, Espoo, FIN-02015 HUT Finland

The measurement of micron-sized mechanical resonators by electrical techniques is difficult, because of the combination of a high frequency and a small mechanical displacement which together suppress the electromechanical coupling. The only electromagnetic technique proven up to the range of several hundred MHz requires the usage of heavy magnetic fields and cryogenic conditions. Here we show how, without the need of either of them, to fully electrically detect the vibrations of conductive nanomechanical resonators up to the microwave regime. We use the electrically actuated vibrations to modulate an LC tank circuit which blocks the stray capacitance, and detect the created sideband voltage by a microwave analyzer. We show the novel technique up to mechanical frequencies of 200 MHz. Finally, we estimate how one could approach the quantum limit of mechanical systems.

PACS numbers: 67.57.Fg, 47.32.-y

Micro- and nanomechanical systems [1, 2] are increasingly finding use in various sensor applications, where the vibrations of clamped beams or cantilevers are affected by the measured quantities. The detection of mechanical vibrations at the submicron scale in such systems gets notoriously difficult. This essentially stems from the fact that the transduction of mechanical motion into the engineering world based typically on *electrical* measurement techniques is not easy. Also, the detection of higher mechanical resonant frequencies f_0 becomes increasingly difficult, since the physical size shrinks roughly inversely with increasing frequency. On the other hand, the smallest nanomechanical resonators are the most interesting ones, as sensors due to their small active mass [3], or, for the benefit of basic research, for observing quantum-mechanical phenomena in the collective mechanical degree of freedom [4, 5].

The backbone for electronic readout of nanomechanical resonators (NR) has been the magnetomotive method [6, 7] or its variants [8] which have been proven above 500 MHz [9]. Here, the current-carrying beam is vibrating in a sizable magnetic field, thus inducing an electromotive force which can be read out by a network analyzer. However, the method has a practical constraint limiting its general applicability, since typically a 1-10 Tesla field and hence superconducting magnets and 4 Kelvin operation are needed.

Apart from simple readout, the most significant motivation for the investigation of sensitive and fast detection methods for NR is the ongoing quest towards experimentally reaching their quantum ground state [10, 11, 12]. The quantum limit necessitates, first of all, a low temperature T such that $hf_0 \gtrsim k_B T$. New materials and fabrication techniques recently paved the way to breaking $f_0 = 1$ GHz [13], corresponding to $T \sim 50$ mK which is relatively easily attainable using standard dilution refrigeration techniques. The prerequisites for the detection method, however, become formidable. The magnetomotive readout appears not suitable for pursuing the

quantum limit, since the high field suppresses superconductivity, which also gives rise to Joule heating. Similarly, a frequently applied piezoelectric actuation may become problematic under these circumstances.

Already from the point of view of practical benefit of either the research scientist or, in particular, for a multitude of high-frequency sensor applications, a straightforward electronic readout would be valuable, which would desirably work up to $f_0 \sim 1$ GHz, and without the use of cumbersome high Tesla magnets. Truitt *et al.* recently took a first step to this direction [14]. They took advantage of the fact that at the drive frequency a driven NR looks like a series electrical RLC resonator, for which they improved the impedance match to $Z_0 = 50 \Omega$ by coupling the NR to an electrical LC matching circuit resonant with the mechanical mode.

In our work, we demonstrate a fully electric readout protocol which uses an external tank circuit in order to eliminate the external wiring capacitances which otherwise would mask the tiny capacitance modulation which comes from the motion of the metallic NR. In the present work, the LC frequency $f_{LC} \gg f_0$ can be chosen high enough to ensure bandwidths up to the range of 1 GHz, independent on f_0 . Similar techniques where an external resonant ("tank", meaning energy storage) circuit have been used in order to enhance the detection bandwidth are well-known in the mesoscopic electron transport community [15, 16, 17]. Estimates show that the method is promising in approaching the quantum limit.

In Fig. 1 (a) we review our starting point, namely the idea of the capacitive actuation and readout, where the NR is driven by the voltage $V(t) = V_{dc} + V_0 \cos(\omega t)$. The NR oscillates as a Lorentzian about the (fundamental mode) mechanical resonance $\omega_0 = 2\pi f_0$:

$$\delta x(\omega, t) = \frac{F_0 \cos(\omega t + \Theta)}{M \sqrt{(\omega \omega_0 / Q_M)^2 + (\omega^2 - \omega_0^2)^2}} \quad (1)$$

where the driving ac-force is $F_0 = \left(\frac{\partial C_R}{\partial x}\right) V_{dc} V_0$, $\tan \Theta =$

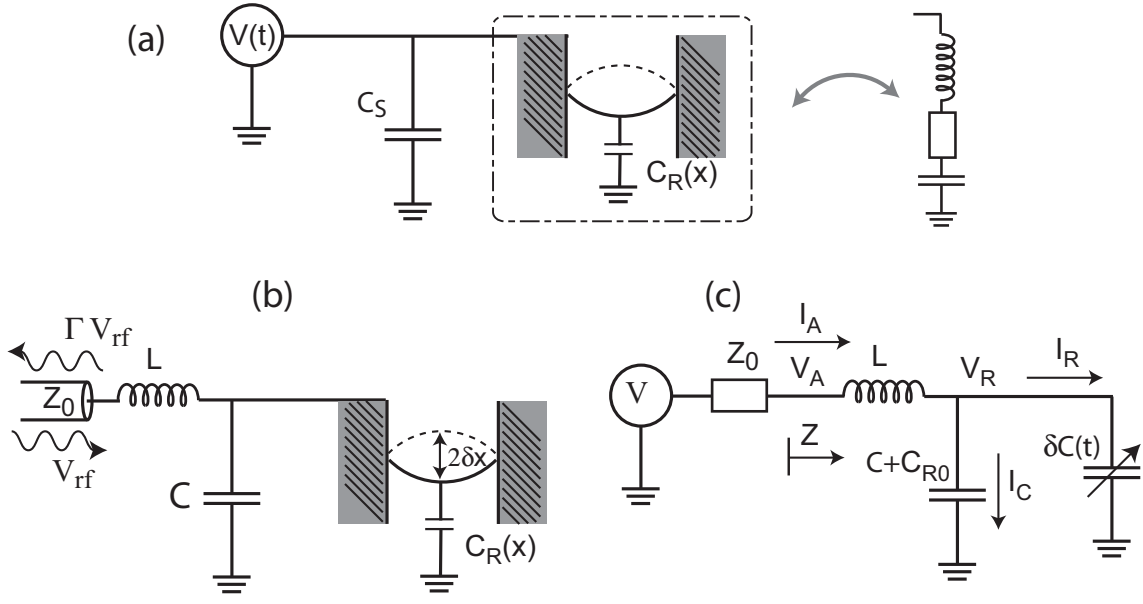


FIG. 1: (a) Capacitive readout of a nanomechanical resonator (without a tank circuit) would suffer from the large parasitic wiring capacitances C_S . The drive $V(t) = V_{dc} + V_0 \cos(\omega_0 t)$ is at mechanical resonance frequency $2\pi f_0$. Inset: electrical equivalent circuit how the mechanical resonator looks like at the same frequency as it is driven. (b) The signal is enhanced in our scheme by a low- Q_{LC} LC tank circuit which blocks the stray capacitance. The vibrations of the beam (driven or not) at the mechanical frequency f_0 modulate the total capacitance of the tank circuit, and the signal occurs as sidebands of the reflected incoming wave $V_{rf} \sin(\omega_{LC} t)$ performed at the frequency $f_{LC} \gg f_0$ of the tank circuit; (c) the circuit appears as one with a time-dependent capacitance when sensed at a frequency different from the actuation frequency f_0 .

$\omega_0 \omega [Q_M (\omega^2 - \omega_0^2)]^{-1}$, M is the effective mass of the fundamental mode (about 0.73 times the total mass of the beam), and Q_M is the quality factor of the nanomechanical mode.

Equation (1) gives rise to a time-varying capacitance $C_R(t) = C_{R0} + \left(\frac{\partial C_R}{\partial x}\right) \delta x$, which at the drive frequency equals the electrical RLC equivalent circuit shown in the inset of Fig. 1 (a).

On the mechanical resonance $\Theta = \pi/2$, current and voltage are in phase and NR looks like a resistance. Towards increasing mechanical frequency, this effective resistance grows rapidly, and when combined with the large wiring stray capacitances C_S , makes the signal small. Truitt *et al.* [14] recently reported a progress which took advantage of the electrical analog augmented with a tank circuit in order to improve the impedance match to $Z_0 = 50 \Omega$.

In order to analyze our approach, Fig. 1 (b), we write down the time-varying capacitance when the NR is resonantly actuated by $V(t) = V_{dc} + V_0 \cos(\omega_0 t)$:

$$\begin{aligned} C_R &= C_{R0} + \delta x \left(\frac{\partial C_R}{\partial x} \right) \sin(\omega_0 t) = \\ &= C_{R0} + \left(\frac{\partial C_R}{\partial x} \right)^2 \frac{V_{dc} V_0 Q_M}{M \omega_0^2} \sin(\omega_0 t) \end{aligned} \quad (2)$$

Here and henceforth, we will denote by δx the resonant (maximum) value of the displacement in Eq. (1). We

perform the measurement at a frequency f_{LC} fully different from the actuation frequency $f \sim f_0$, and as we shall see, this has the effect of erasing the phase relationship between the voltages and currents, and the NR therefore looks just like a time-varying capacitance, as displayed in Fig. 1 (c). At the measurement frequency f_{LC} the RLC equivalent model still holds, but the impedance is such high that its contribution can be neglected. A related technique was recently demonstrated by Regal *et al.* [12], however, they used a very high- Q transmission line resonator as the coupling element, and a low-frequency NR.

For a more thorough analysis, let us write down the equations governing the flow of information between the different frequencies present in the problem, namely the actuation drive to the NR at the frequency f_0 , measurement at $f_{LC} = \frac{1}{2\pi \sqrt{L(C+C_{R0})}}$, and the mixing products (sidebands) $f_{\pm} \equiv f_{LC} \pm f_0$, but neglecting higher-order mixing terms (a related analysis for the RF-SET can be found in Ref. [18]).

The voltages at the various frequencies in the middle of the tank circuit, at the point R in Fig. 1 (c) are, under these assumptions,

$$\begin{aligned} V^R &= V_{dc}^R + V_0^R \exp(i\omega_0 t) + V_{LC}^R \exp(i\omega_{LC} t) + \\ &V_+^R \exp[i(\omega_{LC} + \omega_0)t] + V_-^R \exp[i(\omega_{LC} - \omega_0)t] \end{aligned} \quad (3)$$

Using Eq. (2) for the time-dependent capacitance and Eq. (3) for the voltage across the NR, we get a relation

for the currents I^R flowing through the NR:

$$I^R(t) = \frac{d}{dt} [C_R(t)V^R(t)] \simeq \frac{\delta x \left(\frac{\partial C_R}{\partial x} \right)}{2} \{ \omega_0 V_{dc}^R \exp(i\omega_0 t) + \omega_{LC} (V_+^R - V_-^R) \exp(i\omega_{LC} t) + \omega_+ V_{LC}^R \exp(i\omega_+ t) - \omega_- V_{LC}^R \exp(i\omega_- t) \} + I_{R0} \quad (4)$$

where I_{R0} is the current through the constant part of the capacitance C_{R0} . We use the Kirchoff's voltage and current laws which allow us to solve the circuit at all the mentioned three frequencies, when substituted by Eqs. (3,4):

$$V - I^A (Z_0 + i\omega L) - V^R = 0 \quad (5)$$

$$V^R = \frac{I^A - I^R}{i\omega (C + C_{R0})}$$

If $\omega_0 \ll \omega_{LC}/Q_{LC}$, and in the limit of small capacitance modulation $\delta x \left(\frac{\partial C_R}{\partial x} \right) \ll C_{R0}$, we obtain from Eqs. (5) the measured quantity, namely the voltage amplitudes $V_{\pm} = Z_0 I_{\pm}^A$ of either sideband:

$$V_+ = V_- = \frac{\delta x \left(\frac{\partial C_R}{\partial x} \right) V_{rf}}{2\omega_{LC} (C + C_{R0})^2 Z_0} = \simeq \left(\frac{C_{R0}}{C + C_{R0}} \right)^2 \frac{Q_M V_{dc} V_0 V_{rf}}{2x_0^2 M \omega_{LC} Z_0 \omega_0^2} \quad (6)$$

where for the last form, we substituted the capacitance modulation amplitude δC as defined in Eq. (2), and then approximated it as $\frac{\partial C_R}{\partial x} \sim \frac{C_{R0}}{x_0}$ where x_0 is the vacuum gap between the beam and the gate. As one would intuitively think, the signal depends strongly on how much stray capacitance C one has *within* the resonant circuit, the part which is not cancelled by the inductor. The signal is proportional to both actuation parameters (V_{dc} and V_0) and to how much the system responds, given by Q_M , as well as to the measurement strength V_{rf} . Also, the signal can be interpreted as being proportional to the quality factor $Q_{LC} \sim (\omega_{LC} C Z_0)^{-1}$ of the tank circuit. The bandwidth, as typical of a modulation scheme, is given by the response time of the electrical tank circuit, as f_{LC}/Q_{LC} .

For the fabrication of micron-scale suspended, metallized of fully metallic nanomechanical beams, a multitude of ingenious methods have been developed [7, 9, 19, 20, 21, 22, 23]. Our process represents the simplest end of the spectrum in terms of the complexity of the process, and the number of steps needed. The beam itself is metallic, and hence there is no separate metallization needed. The fabrication goes on top of a high-resistivity ($\sim 3 \text{ k}\Omega\text{m}$) Silicon as shown in Fig. 2, by e-beam lithography. In the end, a properly timed SF_6 dry etch suspends the beam, while leaving the clamps in both ends well hooked to the substrate.

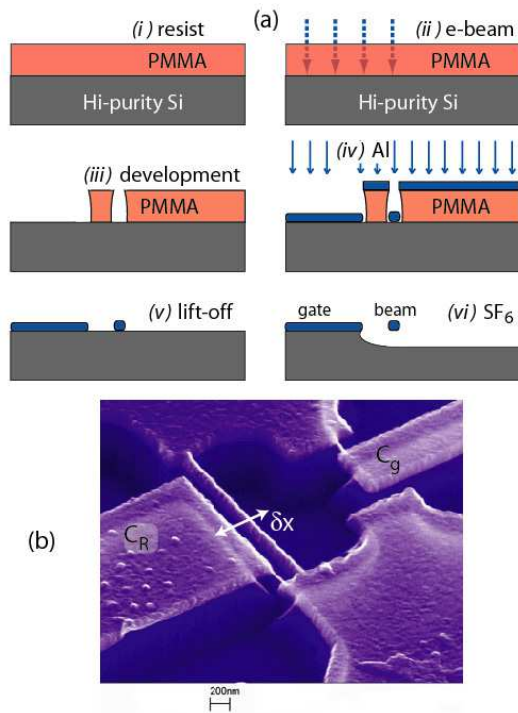


FIG. 2: The fabrication of the nanomechanical resonators on high-resistivity Silicon substrate; (a) the process steps: (i) high-purity Si substrate is coated by 300 nm of PMMA resist; (ii) positive e-beam exposure of the final pattern; (iii) resist development; (iv) e-beam evaporation of a thickness $h = 50 \text{ nm}$ or $h = 100 \text{ nm}$ of Aluminum; (v) lift-off in acetone; (vi) the chip as a whole is exposed to SF_6 Reactive Ion Etch (RIE) which removes $\sim 1 \mu\text{m}$ layer of the Si substrate. (b) SEM image of a $l = 1.8 \mu\text{m}$ long and $W = 160 \text{ nm}$ wide Al beam (similar to samples A and B). The scale bar is 200 nm. The beam is driven to oscillate (amplitude δx) in the plane of the film due to capacitive drive from the large gate C_R . The same gate is also used to sense the motion. The other, weakly coupled, gate C_g was not used presently.

For the measurements, the chip was wire-bonded to a surface-mount inductor $L = 10..30 \text{ nH}$ in a sample holder. The tank circuit capacitance $C \sim 0.3 \text{ pF}$ comes from the stray capacitances of the bonding pad and of the inductor. The choice of the inductor was made such that the expected mechanical frequency falls within the electrical bandwidth $Z_0/(2\pi L)$. The sample was connected to high-frequency coaxial cables in a test cryostat, and cooled down to 4 K in a vacuum of $\sim 10^{-2} \text{ mBar}$. The voltages at dc, at the NR drive frequency, and at the measurement frequency were combined at room temperature using bias tees. The signal reflected from the sample was feed to a spectrum analyzer via a circulator and room temperature microwave amplifiers having the noise temperature $T_N \sim 100 \text{ K}$ which set the noise level in the measurement. The driven mechanical response was obtained by scanning the drive frequency f_g about the mechanical resonance f_0 , and recording the amplitude of

the sideband voltage.

We studied a total of four samples as summarized in Table I for their dimensions, the used tank circuit, and the basic characteristics f_0 and Q_M of the resonance. In Figs. 3, 4 we show more data for two representative samples. As the basic test of the scheme, we compared the measured sideband voltage to that expected, Eq. (6) according to our model of a time-varying capacitance. We model the capacitance C_R between the beam and the nearby gate as that for two parallel beams of length l , width W and a vacuum gap x_0 :

$$C_R(x_0) = \pi\epsilon_0 l \left\{ \ln \left[\frac{x_0}{W} + 1 + \sqrt{\left(\frac{x_0}{W}\right)^2 + \frac{2x_0}{W}} \right] \right\}^{-1} \quad (7)$$

In Figs. 3 (b), 4 (b) we plot the height of the peak obtained as the drive frequency f_g was scanned through the resonance, as a function of the dc voltage. We calculate numerically $\left(\frac{\partial C_R}{\partial x}\right)$ which we use in Eq. (6) in order to obtain the gray lines illustrating the expected linear increase of the peak height, showing a good agreement with the data. The error bars arise from uncertainties in the attenuation of the system at low temperature, as well as uncertainty in the exact value of the beam gap x_0 to which the capacitance is sensitive. Note, however, that all the parameters were independently estimated.

As a further test of integrity of our model, we studied the shift of the linear-regime resonant frequency as a function of the applied dc voltage V_{dc} . Due to electrostatic softening of the effective spring constant $k^*(V_{dc}) = k - \frac{1}{2}V_{dc}^2 \frac{\partial^2 C_R}{\partial x^2} |_{V_{dc}}$, the resonance is expected to shift left with increasing dc voltage:

$$\omega_0(V_{dc}) = \omega_0(0) \left[1 - \frac{C_{R0} V_{dc}^2}{2M\omega_0^2(0)x_0^2} \right] \quad (8)$$

which holds well for the gap smaller than beam diameter. In Figs. 3 (c), 4 (c) we plot the theory prediction together with data as the gray curves which represent Eq. (8) evaluated at opposite limits of the error bars. We notice the match is good to both the magnitude of the frequency shift, as well as its expected quadratic behavior, again without any fitting parameters.

The mechanical frequencies summarized in Table I agree within 25 % of the prediction based on a stress-free film. For samples A and B the measured frequency falls below the predicted, whereas C and D show the opposite. Sample C was briefly heat-treated (see Table I), which could have removed the supposedly compressive stress present in the film after evaporation, thus causing the frequency to go up. The good mechanical Q -values $Q_M > 10^3$, in agreement with previous 4-Kelvin experiments on Aluminum beams [9], do not indicate damage to the beam material was caused by the process.

While our scheme in principle offers room temperature operation, we found out that the (small) conductivity of

the Si substrate caused spurious non-linearities at temperatures above that of liquid nitrogen (77 K), which masked the signal. This issue could be settled by using a more resistive substrate, such as oxidized Silicon.

The fast sideband detection procedure which we demonstrate here offers a sensitive, an in-principle table-top characterization method for the nanomechanical resonators. A major figure of merit is the displacement sensitivity s_x . It is obtained from Eq. (6) as the value of δx which would correspond to a voltage spectral density equal to the noise voltage $\sqrt{2k_B T_N Z_0}$ which we suppose is set by the amplifiers:

$$s_x \simeq 2\sqrt{2k_B T_N Z_0^3 x_0} \frac{\omega_{LC}(C + C_{R0})^2}{C_{R0} V_{rf}} \quad (9)$$

where T_N is the noise temperature of the system. Notice that the sensitivity does not depend on the *actuation* voltages V_{dc} and V_0 , but evidently improves with increasing *measurement* voltage V_{rf} under the assumption that linearity holds. The dependence on the sample dimensions comes via C_{R0} which scales with the length l as $C_{R0} \propto l$. Hence in the "easy" limit where the stray capacitance C dominates, towards small size the sensitivity degrades relatively slowly, as $\propto l^{-2}$. For instance, we expect the method to be usable in order to detect small vibrations for an Al doubly clamped beam of length $l = 0.7 \mu\text{m}$, $f_0 \simeq 1 \text{ GHz}$. Let us use the moderate values $L = 8 \text{ nH}$, $C = 0.1 \text{ pF}$, $T_N = 100 \text{ K}$, $V_{rf} = 3 \text{ mV}$, and $V_{dc} = 10 \text{ V}$, with which values we find a sensitivity of $s_x \sim 0.5 \text{ pm}/\sqrt{\text{Hz}}$.

The sideband readout also seems promising for basic studies of the NR at low temperatures, since the NR and its surroundings stay superconducting. The dispersive detection where only the phase of the reflected signal varies, as well as the all-electric actuation we apply, cause a vanishing on-chip dissipation.

Interestingly, the sideband measurement might also offer a path towards the quantum limit of mechanical motion. Through minimization of the tank circuit capacitance C in Fig. 1 (b) by improving the LC tank circuit from our first realization made of surface mount components, one could approach the sensitivity needed for observing the mechanical zero-point vibrations. The lowest C would be achieved by fabricating the NR coupled to an on-chip spiral coil, for example $L = 17 \text{ nH}$, $C \sim 25 \text{ fF}$. Let us consider an Aluminum beam having a length $l = 1.5 \mu\text{m}$ and frequency $f_0 = 240 \text{ MHz}$. Let us also take $f_{LC} = 5 \text{ GHz}$ and $T_N = 4 \text{ K}$. If probed even with a decent $V_{rf} = 3 \text{ mV}$, and $V_{dc} = 10 \text{ V}$, Eq. (9) yields a displacement sensitivity $s_x \sim 45 \text{ fm}/\sqrt{\text{Hz}}$, which comes interestingly close to the zero-point amplitude $x_{zp} \sim 25 \text{ fm}$ whose energy will be spread over a bandwidth determined by Q_M . The back-action disturbance due to the probing remains small, since $f_{LC} \gg f_0$. The back-action is estimated from the tail of the Lorentzian response of Eq. (1), where the amplitude at high frequencies decays

TABLE I: List of the measured nanomechanical resonators. They were fabricated out of Al according to Fig. 2. Sample C was baked in vacuum at 200°C for 15 min. The quality factors Q_M and the fundamental mode resonance frequencies f_0 were measured in a temperature of 4.2 K in a vacuum of $\sim 10^{-2}$ mBar. The estimated frequency is given as $f_0 \simeq \frac{W}{l^2} \sqrt{\frac{E}{\rho}}$, where E is the Young modulus and ρ is density. The other beam parameters are l = length, W = width, h = thickness, x_0 = vacuum gap.

sample	l	W	h	x_0	f_0 (est)	f_0 (meas)	L	C_R	C	f_{LC}	Q_M
A	1.8 μm	150 nm	100 nm	65 nm	230 MHz	172 MHz	20 nH	47 aF	0.39 pF	1.81 GHz	1.0×10^3
B	1.8 μm	160 nm	50 nm	70 nm	245 MHz	191 MHz	14 nH	45 aF	0.27 pF	2.16 GHz	1.0×10^3
C	2.2 μm	200 nm	75 nm	100 nm	205 MHz	202 MHz	10 nH	64 aF	0.3 pF	3.02 GHz	1.0×10^3
D	2.5 μm	145 nm	150 nm	170 nm	117 MHz	130 MHz	10 nH	49 aF	0.3 pF	2.95 GHz	2.6×10^3

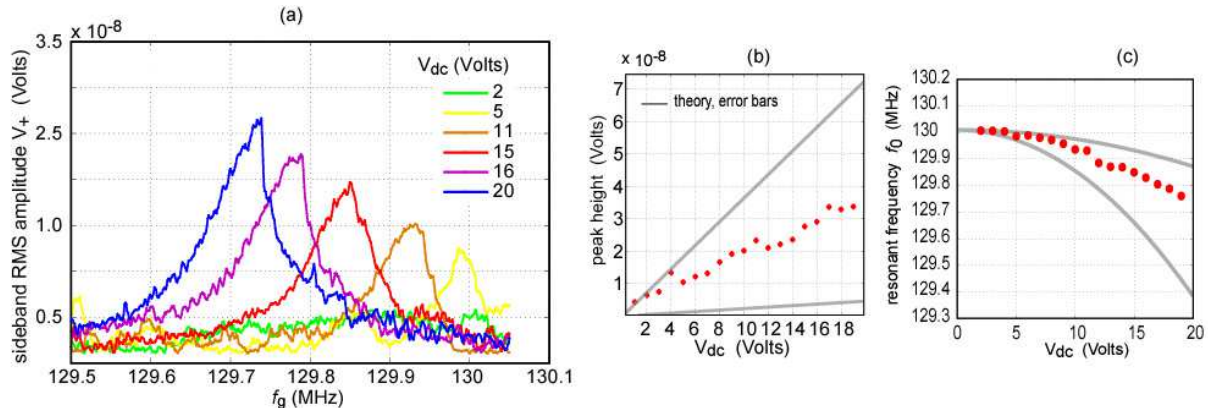


FIG. 3: Measurements of the response of the nanomechanical resonator (sample D) using the electric sideband detection, $V_0 = 100$ mV and $V_{LC} = 30$ mV, at $T = 4.2$ K; (a) resonance curves of the fundamental mode for increasing dc voltage (from right to left); (b) Amplitude of the peak extracted from (a). The theoretical predictions (gray lines) are scaled down by the total microwave attenuation ~ 10 dB of the system; (c) center frequency of the mechanical peak extracted from (a), compared to theory from Eq. (8);

as $(f_{LC})^{-3}$. With the above parameter values, we find that the measurement would excite less than one quantum of energy into the NR.

An interesting materials platform for the sideband readout, among all conductive materials, is graphene [24]. The signal improves due to a large capacitance of the sheet and due to its low mass, whereas the latter also substantially increases the zero-point amplitude. Due to the sensitivity of the novel method, interesting mass, acceleration or other sensor applications might also arise.

We wish to acknowledge Jukka Pekola, Sami Franssila and Antti O. Niskanen for useful discussions. This work was supported by the Academy of Finland, and by EU contract FP6-021285.

* Electronic address: Mika.Sillanpaa@iki.fi

- [1] A. Cleland, *Foundations of Nanomechanics* (Springer, New York, 2003).
- [2] K. L. Ekinci and M. L. Roukes, *Rev. Sci. Instrum.* **76**, 061101 (2005).
- [3] K. Jensen, K. Kim, and A. Zettl, *Nature Nanotech.* **3**,

- 533 (2008).
- [4] E. K. Irish and K. Schwab, *Phys. Rev. B* **68**, 155311 (2003).
- [5] A. N. Cleland and M. R. Geller, *Phys. Rev. Lett.* **93**, 070501 (2004).
- [6] D. S. Greywall, B. Yurke, P. A. Busch, A. N. Pargellis, and R. L. Willett, *Phys. Rev. Lett.* **72**, 2992 (1994).
- [7] A. N. Cleland and M. L. Roukes, *Appl. Phys. Lett.* **69**, 2653 (1996).
- [8] K. L. Ekinci, Y. T. Yang, X. M. H. Huang, and M. L. Roukes, *Appl. Phys. Lett.* **81**, 2253 (2002).
- [9] T. F. Li, Y. A. Pashkin, O. Astafiev, Y. Nakamura, J. S. Tsai, and H. Im, *Appl. Phys. Lett.* **92**, 043112 (2008).
- [10] M. D. LaHaye, O. Buu, B. Camarota, and K. C. Schwab, *Science* **304**, 74 (2004).
- [11] A. Naik, O. Buu, M. D. LaHaye, A. D. Armour, A. A. Clerk, M. P. Blencowe, and K. C. Schwab, *Nature* **443**, 193 (2006).
- [12] J. D. Regal, C. A. Teufel, and K. W. Lehnert, *Nature Physics* **4**, 555 (2008).
- [13] X. M. H. Huang, C. A. Zorman, M. Mehregany, and M. L. Roukes, *Nature* **421**, 496 (2003).
- [14] P. A. Truitt, J. B. Hertzberg, C. C. Huang, K. L. Ekinci, and K. C. Schwab, *Nano Lett.* **7**, 120 (2007).
- [15] R. Schoelkopf, P. Wahlgren, A. Kozhevnikov, P. Delsing, and D. Prober, *Science* **280**, 1238 (1998).

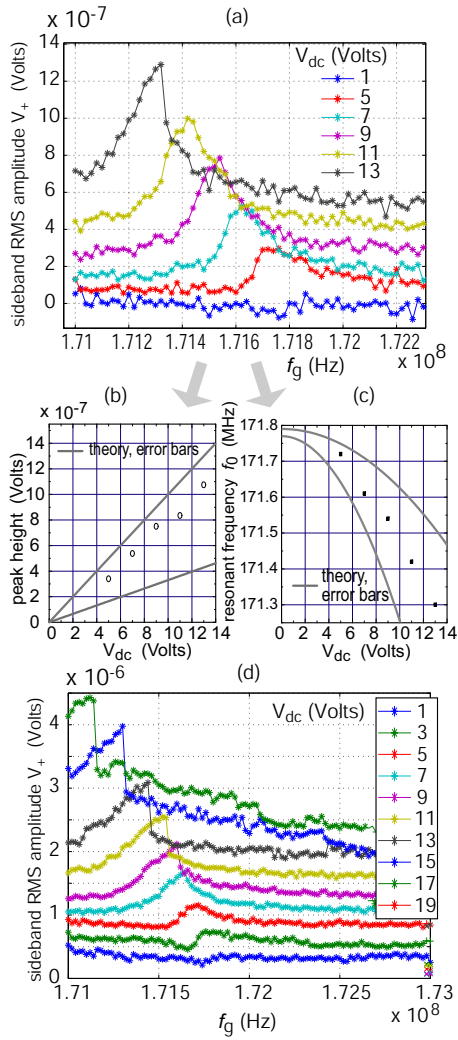


FIG. 4: As Fig. 3; measurement and analysis for sample A; (a) $V_0 = 50$ mV and probe $V_{LC} = 140$ mV, for increasing values of the dc voltage V_{dc} from bottom to top (displaced vertically for clarity); (b) increase of the height of the peak versus dc voltage; (c) frequency shift versus dc voltage; (d) at a higher total drive $V_0 = 50$ mV and $V_{LC} = 200$ mV, the system turns nonlinear and hysteretic.

- [16] L. Roschier, M. Sillanpää, and P. Hakonen, Phys. Rev. B **71**, 024530 (2005).
- [17] M. Sillanpää, L. Roschier, and P. Hakonen, Phys. Rev. Lett. **93**, 066805 (2004).
- [18] L. Roschier, M. Sillanpää, T. Wang, M. Ahlskog, S. Iijima, and P. Hakonen, Journal of Low Temperature Physics **136**, 465 (2004).
- [19] A. N. Cleland, M. Pophristic, and I. Ferguson, Appl. Phys. Lett. **79**, 2070 (2001).
- [20] Y. T. Yang, K. L. Ekin, X. M. H. Huang, L. M. Schiavone, M. L. Roukes, C. A. Zorman, and M. Mehregany, Appl. Phys. Lett. **78**, 162 (2001).
- [21] A. Husain, J. Hone, H. W. C. Postma, X. M. H. Huang, T. Drake, M. Barbic, A. Scherer, and M. L. Roukes, Appl. Phys. Lett. **83**, 1240 (2003).
- [22] L. Sekaric, J. M. Parpia, H. G. Craighead, T. Feygelson, B. H. Houston, and J. E. Butler, Appl. Phys. Lett. **81**, 4455 (2002).
- [23] V. Sazonova, Y. Yaish, T. A. H. Üstünel, D. Roundy, and P. McEuen, Nature **431**, 284 (2004).
- [24] J. S. Bunch, A. M. van der Zande, S. S. Verbridge, I. W. Frank, D. M. Tanenbaum, J. M. Parpia, H. G. Craighead, and P. L. McEuen, Science **315**, 490 (2007).